J Supercond Nov Magn (2016) 29:343–347
DOI 10.1007/s10948-015-3231-2

ORIGINAL PAPER

# Fabrication of $Co_2Ni_8$/CNTs Alloy Hollow-nanostructured Microspheres: Facile Synthesis and Magnetic Properties

**Xiuting Wang[1] · Zhanyong Wang[1] · Wenya Yang[1] · Tianpeng Wang[1] · Qizhong Chen[1]**

Received: 21 September 2015 / Accepted: 26 September 2015 / Published online: 21 October 2015


**Abstract** $Co_2Ni_8$ hollow-nanostructured microspheres were synthesized by template-free hydrothermal method at 150 °C. Mixing of the carbon nanotubes (CNTs) and $Co_2Ni_8$, $Co_2Ni_8$/CNTs can be attained at 400 °C after vacuum heat treatment. The amorphous nature of these powders was confirmed by various techniques, such as X-ray diffraction (XRD), scanning electron microscopy (SEM), and vibrating sample magnetometer (VSM). An SEM of heated $Co_2Ni_8$ sample showed near-uniform particles with sizes of 15$\mu$m. The observed magnetization of the $Co_2Ni_8$/CNTs (59.40 emu/g) was lower than that of $Co_2Ni_8$ (97.10 emu/g) with VSM. However, the coercivity ($H_c$) (24 Oe) and saturation magnetization ($M_s$) (145.00 emu/g) of Co/CNTs were better than those of Co (150 Oe, 80.80 emu/g).

**Keywords** Hydrothermal method · Hollow-nanostructured · Magnetic properties · Cobalt-nickel

## 1 Introduction

Nanostructures of binary metallic alloys have attracted intensive attention by researchers owing to their excellent properties and technological application in diverse fields. Among magnetic metals, $Co_2Ni_8$ is attractive due to their magnetic and catalytic properties for application in magnetic recording media [1], sensors [2], hydrogen storage application [3], and catalysts [4]. Nanosized $Co_2Ni_8$ particles have been synthesized by various methods, including liquid phase reduction method [5], sonochemical method [6], electrodeposition method [7], microemulsion method [8], precursors method [9], mechanical alloying [10], polyol reduction method [11, 12], and hydrothermal routes method [13]. In the past decades, diverse assembled structures have been synthesized by different ways, such as nanowires [14, 15], flowery particles [16], nanodumbbells [17], chain-like [18], and sphere [19]. Owing to their sizes, morphology, and composition-dependent properties, $Co_2Ni_8$ nanomaterials with controllable sizes, shapes, dimensions, and different molar ratios are highly desirable for different applications, especially the $Co_2Ni_8$ alloy hollow-nanostructured microspheres.

In recent years, the kinds of $Co_2Ni_8$ alloy with special structure and morphology have been the subject of widespread interest, especially the application of hollow nanospheres. A hollow ball is evolved by core-shell composite structure materials, owing to the composite core-shell different components [20] and the common characteristics of coordination between the various components, so the structure, size, and composition of core-shell composite particles can be adjusted to control their corresponding properties, so as to realize the optical, thermal, electrical, mechanical, magnetism, catalysis, and so on in a wide range of applications. Because of this kind of structure material with low density, high specific surface, high surface activity, high permeability, and high stability of the features, the hollow nanosphere materials have some peculiar

✉ Zhanyong Wang
wang092688@sina.cn

[1] Department of Material Science and Engineering, Shanghai Institute of Technology, Shanghai 201418, China

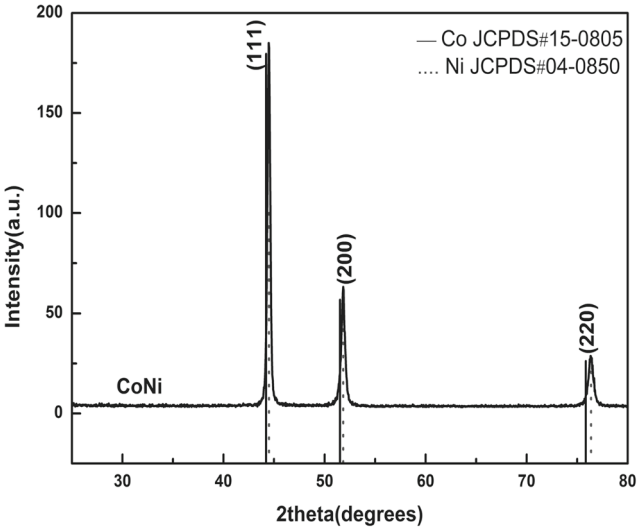


**Fig. 1** The XRD patterns of $Co_2Ni_8$

applications like micro package, drug delivery, magnetic storage, solar photovoltaic cells, biological material, chemical storage, low dielectric constant material, catalyst, adsorbent, and sensors.

Carbon nanotubes (CNTs) have been considerably researched due to their small density and excellent physical and chemical properties [21]. CNTs could increase the toughness and thermal stability of $Co_2Ni_8$ and Co. Recently, many researchers have studied the CNTs, SiC/CNTs and $SiO_2$/CNTs [22, 23]. However, to the best of our knowledge, there are few studies on the magnetic properties of $Co_2Ni_8$/CNTs alloy hollow-nanostructured microspheres so far.

In this report, a traditional reduction method, which is commonly used in the synthesis of ferrite materials, was used. The $Co_2Ni_8$ alloy hollow-nanostructured microspheres have been synthesized by hydrothermal method with an easy processing and low temperature. $Co_2Ni_8$/CNTs are attained after vacuum heating treatment. Based on the measurement results, the magnetic property of $Co_2Ni_8$/CNTs has been studied.

## 2 Experimental

Cobalt(II) chloride hexahydrate ($CoCl_2 \cdot 6H_2O$), nickel(II) chloride hexahydrate ($NiCl_2 \cdot 6H_2O$), hydrazine monohydrate ($N_2H_4 \cdot H_2O$, 85 %), and $NH_3$ solution (25–28 % of analytical grade were purchased from Sinopharm Chemical Reagent Co., Ltd. Firstly, 30 mmol of $CoCl_2 \cdot 6H_2O$ and 120 mmol of $NiCl_2 \cdot 6H_2O$ were dissolved in 20 mL of deionized water, then stirred strongly for 20 min to form a homogenous solution. Secondly, 20 mL $NH_3$ solution (25–28 %) was added dropwise into the above solution under magnetic stirring. The resultant mixture was stirred vigorously for 20 min. Subsequently, 10 mL hydrazine monohydrate ($N_2H_4 \cdot H_2O$, 85 %) was added to the solution as a reducing agent. The mixture was stirred again for 10 min. Finally, the obtained solution was transferred into a Teflon-lined autoclave with a 100 mL capacity. The temperature was maintained at 150 °C for a certain time (14, 17, 22, and 24 h). Then, it was cooled down to room temperature naturally. The resulting grey products were filtered, washed with deionized water and absolute ethanol, and then dried in the oven at 70 °C overnight.

The crystal structure of powders was measured by D/max-2000 X-ray diffraction measurement with Cu K$\alpha$ radiation ($\gamma$ value of 1.5406 Å). The volume percent of the phases was estimated on the basis of the highest intensity of the diffraction peaks for different phases from the X-ray diffraction (XRD) patterns. In this work, the relative area of the peaks with $2\theta = 44.3°$ , 51.6° and 76.2° was selected, corresponding to (111), (200) and (220) for $Co_2Ni_8$ phases, respectively. The magnetic properties were measured by the Lake Shore 7400 vibrating sample magnetometer (VSM) with a maximum applied magnetic field of 1.0 T at room

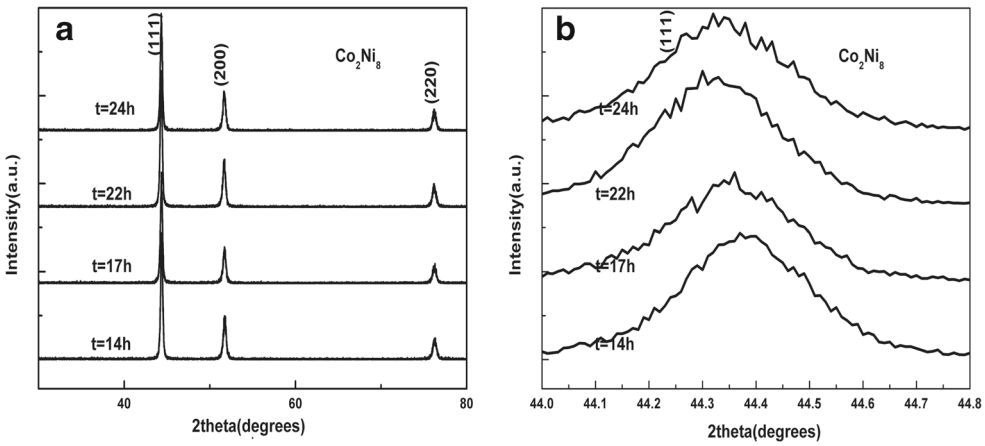


**Fig. 2** **a** The XRD patterns of $Co_2Ni_8$ at different reaction times; **b** the (111) diffraction peaks of $Co_2Ni_8$ at the different times

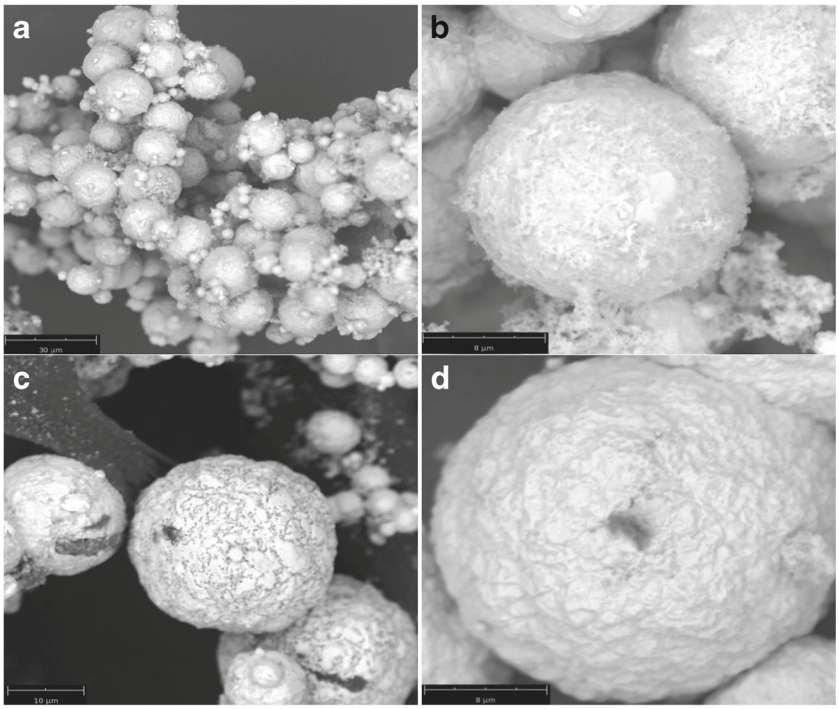


**Fig. 3** SEM images of $Co_2Ni_8$ microstructures with different times. **a** 12 h; **b** 17 h; **c** 22 h; **d** 24 h

temperature. The microstructure was investigated by Phenom Pro Desktop scanning electron microscopy.

## 3 Results and Discussion

Figure 1 shows the XRD patterns of $Co_2Ni_8$ powders by hydrothermal method at 150 °C. All the samples show a strong diffraction peak of $Co_2Ni_8$ phase Three peaks at $2\theta = 44.5°$, 51.6° and 76.2° can be observed in the XRD pattern, corresponding to the (111), (200) and (220) planes of face-centered cubic (fcc) phase $Co_2Ni_8$ alloy [24], which is between face-centered cubic (fcc) nickel (JCPDS: 04-0850) and face-centered cubic cobalt structure (fcc) (JCPDS: 150806), closed to face-centered cubic (fcc) nickel (JCPDS: 04-0850). Since the impurities of $Ni(OH)_2$ or $Co(OH)_2$ are detected in the XRD pattern other characteristic peaks cannot be found in Fig. 1, which indicates that the reduction completed and the powder is pure metal alloy.

**Table 1** Average crystallite size of $Co_2Ni_8$ with different times ($t$ = 12, 17, 22, and 24 h)

| | $t = 12$ h | $t = 17$ h | $t = 22$ h | $t = 24$ h |
|---|---|---|---|---|
| $D$ (nm) | 27.763 | 43.083 | 46.809 | 50.808 |

Figure 2a shows the XRD patterns of $Co_2Ni_8$ powders at different reaction times. Figure 2b shows that the peak of (111) shifts to small angle with the time, which may be caused by the lattice distortion. $Co^{2+}$ ion reduces to Co, then infiltrates the interstices of Ni. The atomic radius of Ni is smaller than that of Co, so the diffraction angle shifts to the small angle according to the Bragg formula. Figure 2b indicates Co infiltrates the interstices of Ni completely at 22 h.

Figure 3a, b shows the particle diameter of $Co_2Ni_8$ microspheres is about 10 $\mu$m with an unsmooth surface at 12 h; the hollow microspheres are formed at 21 h of the experiment. Figure 3c, d shows the scanning electron microscopy (SEM) of $Co_2Ni_8$, which indicates that the obtained products are hollow microspheres with a uniform diameter of 27 $\mu$m in the 24h experiment. This phenomenon in which the nano/microspheres are gradually turned into the hollow nano/microspheres was first found by Zeng H. C. [25]. The Ostwald ripening which is also named the second-phase particle coarsening can be explained by the phenomenon. In the process of crystal maturating, monomers are almost run out in the system; the crystal will continue to grow in this way. Monomer small particles in the system have high surface energy, but larger particles have low surface energy, so the small particles dissolve as the monomer to provide fuel for the growth of large particles for the lowest energy. From the point of dynamics, this growth rate of small particles which are dissolved is negative, and the

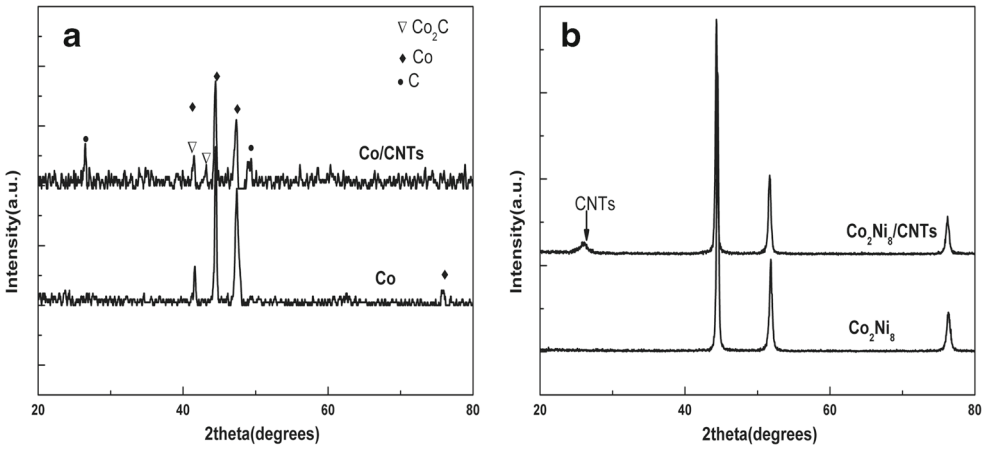


**Fig. 4** The XRD patterns of **a** Co/CNTs and **b** $Co_2Ni_8$/CNTs

growth rate of large particles which are becoming big is positive. From the whole process, the process of the particle size distribution will become wide, but the premise of the slaking mechanism is that the monomer has been completely consumed. Thomson Gibbs equation is the basis of the theory of classical crystallography.

$$S_r = S_b \exp\left(\frac{2\sigma V_m}{rRT}\right) \quad (1)$$

where $r$ is the radius of the crystal size, $\sigma$ is the specific surface area, $V_m$ is the molar volume of material, $R$ is the universal of the gas, $T$ is the degree Kelvin, $S_r$ is the bulk phase materials, and $S_b$ is the solubility of the crystal when the size of bulk phase materials is $r$. So the formula shows that the solubility of a small-size nanocrystalline is big. So small nanocrystals have a tendency of turning into big nanocrystals with time.

Table 1 lists the average crystallite size of $Co_2Ni_8$ with different times. The following Scherrer formula is applied to calculate the average crystallite size $D$.

$$D = K\gamma / B\cos\theta \quad (2)$$

where $D$ is the average crystallite size in the vertical direction of the lattice plane, $K$ is the Scherrer constant, $B$ is the half high width of the sample diffraction peak, $\theta$ is the diffraction angle, $\gamma$ is the X-ray wavelength (0.154056), and shape factor $K$ equals 0.89 for $Co_2Ni_8$.

In Fig. 4 are the XRD of Co/CNTs and $Co_2Ni_8$/CNTs which can be obtained through vacuum heating treatment at 400 °C. The peak at $2\theta$ value of 26.2° is carbon nanotubes. It indicates carbon nanotubes are attached on the surface of $Co_2Ni_8$ without entering into the lattice interstitial position like Fig. 4b. Figure 4a shows the Co has been turned Co/CNTs and contained three phases, Co (JCPDS: 15-0806), C (JCPDS: 41-1487), and $Co_2C$ (JCPDS: 50-1371) after vacuum heating treatment.

Magnetic properties of the samples were investigated at room temperature (300 K) using a VSM with 1T and the results are shown in Fig. 5. In Fig. 5a, the coercivity ($H_c$) and saturation magnetization ($M_s$) of $Co_2Ni_8$ are 60 Oe and 97.10 emu/g respectively. Figure 5b shows that the coercivity ($H_c$) and saturation magnetization ($M_s$) of $Co_2Ni_8$/CNTs are 40 Oe and 59.40 emu/g. The imperfection of the $Co_2Ni_8$/CNTs' crystalline structure at the hollow-nanostructured microspheres' surfaces may also lead to a

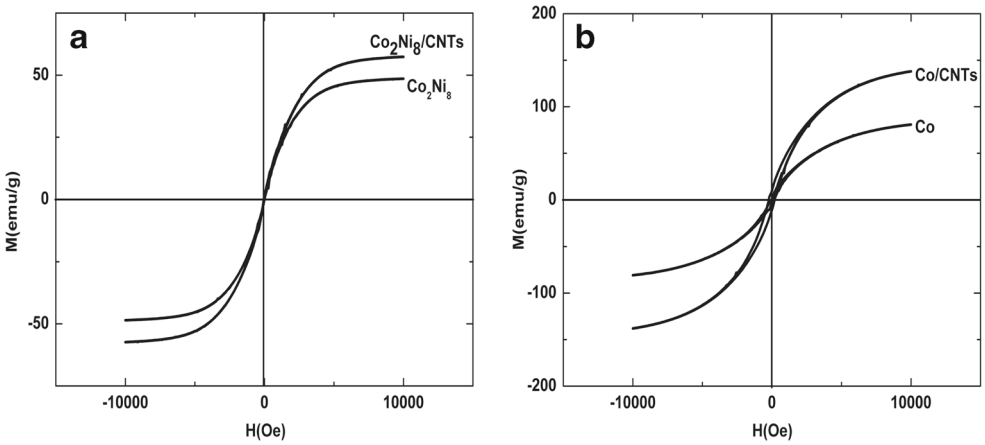


**Fig. 5** **a** The hysteresis loops of $Co_2Ni_8$ and $Co_2Ni_8$/CNTs with 1T at 300 K; **b** the hysteresis loops of Co and Co/CNTs with 1T at 300 K

significant reduction in the saturation magnetization [26]. However in Fig. 5c d the results of Co are different from those of $Co_2Ni_8$; for Co, $H_c$ and $M_s$ are 150 Oe and 80.80 emu/g, but for Co/CNTs, they are 24 Oe and 145.00 emu/g respectively, which indicate that the Co/CNTs are ferromagnetic at room temperature. We also synthesize the $Co_{1-x}Ni_x$ ($x = 0, 0.5, 0.6, 0.8$) with the same method, finding the $M_s$ increases with the increase of Co concentration It may be explained that the magnetic moment of Co and Ni is 2.07 and 0.98 $\mu_B$/atom, respectively and the anisotropy constant has been changed. The addition of CNTs results in the destruction of the symmetry of cobalt; the Co/CNTs' magnetic properties can become better by changing the anisotropy constant. Besides $Co_2C$ has a low magnetic moment but high coercivity. Through firstprinciples calculations, it can be concluded that carbon increases the anisotropy of individual phases, playing a similar role to samarium or neodymium in current rare earth permanent magnets [27]. However the $Co_2Ni_8$/CNTs have the opposite result because the magnetocrystalline anisotropy constant of nickel is negative and its crystal texture has different types.

## 4 Conclusion

In conclusion, we successfully synthesized $Co_2Ni_8$ alloy with hollow-microstructured microspheres through a facile hydrothermal method under 150 °C in the work. Then, $Co_2Ni_8$/CNTs and Co/CNTs can be obtained after vacuum heating treatment. The reaction time is proved to be an important parameter for morphology. The hollow-nanostructured microspheres can be found after 17 h of heating treatment. $Co_2Ni_8$/CNTs and $Co_2Ni_8$ all microcrystalline alloys exhibit superparamagnetic behavior with negligible coercivity and saturation magnetization at 300 K However Co/CNTs' magnetic properties are better than those of Co The result demonstrates that Co/CNTs' powers are promising for magnetic storage and the ultra-high-density magnetic recording application.

**Acknowledgments** This work was supported by the Project of the Shanghai Education Commission of the People's Republic of China (14ZZ165 and J51504) and State Key Laboratory for Advanced Metals and Materials of the People's Republic of China (2013-Z02).

## References

1. Soumare, Y., Piquemal, J.Y., Maurer, T., Chaboussant, G., Ott, F., Falqui, A., Viau, G.: J. Mater. Chem. **18**(46), 5696 (2008)
2. Winnischofer, H., Rocha, T.C., Nunes, W.C., Socolovsky, L.M., Knobel, M., Zanchet, D.: Acs. Nano. **2**(6), 1313 (2008)
3. Rafique, M.Y., Pan, L., Iqbal, M.Z., Qiu, H., Farooq, M.H., Guo, Z., Ellahi, M.: J. Nanopart. Res. **15**(7), 1768 (2013)
4. Sun, L.F., Mao, J.M., Pan, Z.W., Chang, B.H., Zhou, W.Y., Wang, G., Xie, S.S.: Appl. Phy. Lett. **74**(5), 644 (1999)
5. Lu, W., Sun, D., Yu, H.: J. Alloys Comp. **229**, 546 (2013)
6. Kapoor, S., Salunke, H.G., Tripathi, A.K., Kulshreshta, S.K., Mittal, J.P.: Mater. Res. Bull. **35**(1), 143 (2000)
7. Gomez, E., Pane, S., Valles, E.: Electrochim. Acta. **51**(1), 146 (2005)
8. Ahmed, J., Sharma, S., Ramanujachary, K.V., Lofland, S.E., Ganguli, A.K.: J. Colloid. Interface. Sci. **336**(2), 814 (2009)
9. Panday, S., Daniel, B.S.S., Jeevanandam, P.: J. Magn. Magn. Mater. **323**(17), 2271 (2011)
10. Olvera, S., Sánchez-Marcos, J., Palomares, F.J., Salas, E., Arce, E.M., Herrasti, P.: Mater. Character **79**, 93 (2014)
11. Liu, Q., Guo, X., Wang, T., Li, Y., Shen, W.: Mater. Lett. **64**(11), 271 (2010)
12. Guo, X.H., Li, Y., Liu, Q.Y., Shen, W.J., Chin, J.: Catal. **33**(4), 645 (2012)
13. Li, H., Liao, J., Feng, Y., Yu, S., Zhang, X., Jin, Z.: Mater. Lett. **67**(1), 346 (2012)
14. Pan, S., An, Z., Zhang, J., Song, G.: Mater. Lett. **64**(3), 453 (2010)
15. Soumare, Y., Garcia, C., Maurer, T., Chaboussant, G., Ott, F., Fievet, F., Viau, G.: Adv. Funct. Mater. **19**(12), 1971 (2009)
16. Ung, D., Soumare, Y., Chakroune, N., Viau, G., Vaulay, M.J., Richard, V., Fiévet, F.: Chem. Mater. **19**(8), 2084 (2007)
17. Pan, S., An, Z., Zhang, J., Song, G.: Mater. Chem. Phy. **124**(1), 342 (2010)
18. Nie, D., Xu, C., Chen, H., Wang, Y., Li, J., Liu, Y.: Mater. Lett. **131**, 306 (2014)
19. Liu, X.M., Fu, S.Y., Huang, C.J.: Mater. Lett. **59**(28), 3791 (2005)
20. Cao, Zhang, X., Zhu, Y., Ji, Y.: Guangzhou Chem. **40**(11), 3 (2012)
21. Xiang, J., Zhang, X., Ye, Q., Li, J., Shen, X.: Mater. Res. Bull. **60**, 589 (2014)
22. Feng, W., Zhang, L., Liu, Y., Li, X., Cheng, L., Zhou, S., Bai, H.: (2015). Mater. Sci. Eng., A
23. Guo, S., Sivakumar, R., Kagawa, Y.: Adv. Eng. Mater. **9**(1-2), 84 (2007)
24. Zhu, L.P., Xiao, H.M., Fu, S.Y.: Eur. J. Inorg. Chem. **25**, 3947 (2007)
25. Yang, H.G., Zeng, H.C.: J. Phys. Chem. B **108**(11), 3492 (2004)
26. Barakat, N.A.M., Abadir, M.F., Nam, K.T., Hamza, A.M., Al-Deyab, S.S., Baek, W.I., Kim, H.Y.: J. Mater. Chem. **21**, 10957 (2011)
27. Carroll, K.J., Huba, Z.J., Spurgeon, S.R., Qian, M., Khanna, S.N., Hudgins, D.M., Taheri, M.L., Carpenter, E.E.: Appl. Phy. Lett. **101**(1), 012409 (2012)